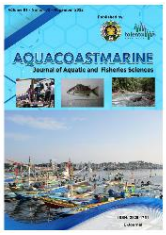
talenta PUBLISHER

AQUACOASTMARINE
Journal of Aquatic and Fisheries Sciences
Journal homepage: https://talenta.usu.ac.id/aquacoastmarine



Shoreline Dynamics and Hydrodynamic Forcing: A 40 Years Analysis of Trends and Response in Jepara, Central Java

Dinamika Garis Pantai dan Gaya Hidrodinamik: Analisis Tren dan Respons Selama 40 Tahun di Jepara, Jawa Tengah

Koko Ondara[1,2], Anindya Wirasatriya[3], Johan Risandi[2], Elis Indrayanti[3], Sayed Ahmad Zaki Yamani[5], Ulung Jantama Wisha[2], Aris Ismanto[3,6*]

[1]Doctoral Program of Marine Science, Marine Science and Fisheries Faculty, Diponegoro University, Semarang 50275 Telp/Fax. 024-7474698
[2]Research Center for Oceanology, National Research and Innovation Agency, Jakarta, Indonesia
[3]Department of Oceanography, Faculty of Fisheries and Marine Science, Diponegoro University, Indonesia
[4]Department of Marine Science, Faculty of Fisheries and Marine Sciences, Universitas Diponegoro Jl. Prof. Jacub Rais, Tembalang Semarang Central Java, 50275, Indonesia
[5]Almuslim University, Bireuen Regency, Aceh Province 24261, Indonesia
[6]Center for Integrated Coastal Zone Management (ICZM Center), Diponegoro University, Semarang, Indonesia
[*]Corresponding author email: koko003@brin.go.id

ARTICLE INFO

Article history:
Received 23 April 2026
Revised 22 June 2026
Accepted 01 November 2026
Available online 14 November 2026

E-ISSN: 2829-1751

How to cite:
Ondara, K., Wirasatriya, A., Risandi, J., Indrayanti, E., Yamani, S. A. Z., Wisha, U. J., Ismanto, A. (2026). Shoreline Dynamics And Hydrodynamic Forcing: A 40 Years Analysis of Trends and Response In Jepara, Central Java. *AQUACOASTMARINE: J.Aquat.Fish.Sci*,, 5(2), 206–217.

ABSTRACT

The shoreline of Jepara Regency, the northern coast of Java, is undergoing transformation due to the incessant movement of oceanic hydrodynamic forces. This study investigates the impact of hydrodynamic conditions on the stability of the Jepara coast over 40 years (1985-2025) and aims to quantify the magnitude and rate of shoreline alterations. Changes along the shoreline using satellite images and interval transect method. EPR, NSM, and SCE methods were used. Monthly average data from the European Center for Medium Range Weather Forecasts satellite to look at the tide, height, and wave period. The study results show that the shoreline is mostly losing land, with a total loss of 12.18 hectares. The land area lost due to cumulative abrasion was -22.33 hectares, which is much greater than the land area gained through accretion, which was only 10.15 hectares. The Ujungtumpuk area on the headland of the northern area is where the coast is most damaged. On the other hand, accretion happens in the middle and southern parts of the country, where the coast looks like a bay. The sea surface temperatures are rising, the water expands and the sea level rises, which makes this abrasion worse. It has been demonstrated that natural land development processes are significantly weaker than detrimental external forces.

Keyword: Hydrodynamic, Jepara, satellite imagery, shoreline changes

ABSTRAK

Kabupaten Jepara yang terletak di Pantai Utara Jawa, mengalami proses perubahan garis pantai sepanjang tahun. Penelitian ini bertujuan untuk mengukur luasan dan laju perubahan garis pantai serta menganalisis pengaruh kondisi hidrodinamika terhadap stabilitas pesisir Jepara selama periode 40 tahun (1985-2025). Perubahan garis pantai sepanjang dianalisis menggunakan data citra satelit dengan metode transek berinterval melalui pendekatan EPR, NSM, dan SCE. Data pasang surut, tinggi, dan periode gelombang dianalisis menggunakan data rerata bulanan dari satelit *The European Center For Medium-Range Weather Forecasts*. Hasil analisis menunjukkan bahwa pesisir Jepara secara umum mengalami penyusutan daratan dengan kehilangan wilayah pesisir bersih sebesar kurang lebih 12,18 hektar. Luasan daratan yang hilang akibat abrasi mencapai 22,33 hektar, sedangkan proses akresi hanya mencapai 10,15 hektar. Laju kemunduran pantai paling destruktif terpusat pada area tanjung di semenanjung utara. Sebaliknya, akresi terjadi pada area pertengahan hingga selatan yang memiliki bentuk garis pantai melengkung menyerupai teluk. Abrasi tersebut diperparah oleh tren pemanasan global, di mana peningkatan suhu permukaan laut berdampak pada kenaikan muka air laut yang membuat gelombang memiliki jangkauan hantaman yang lebih jauh ke daratan. Gaya eksternal yang destruktif terbukti bekerja jauh lebih kuat dibandingkan proses alamiah pembentukan daratannya.

Kata kunci: Hidrodinamika, Jepara, Citra satelit, Perubahan garis pantai

This work is licensed under a Creative Commons Attribution-ShareAlike 4.0 International.
10.32734/jafs.v5i2.25326

1. Introduction

The shoreline in Java's northern coastal region undergoes two changes: abrasion and accretion (Irsadi et al., 2022; Ondara et al., 2018). These changes are a type of coastal geomorphological response to the constant interaction of many ocean hydrodynamic forces (Riptanti et al., 2025). Some of the hydrodynamic forces that affect the movement of sediment along the coast include tides, changes in sea surface temperature, and characteristics of waves and currents (Ondara et al., 2022; Solihuddin et al., 2021; Umar et al., 2025). Global climate change worsens the pressure on the coast. Thermal expansion, or the increase in water volume, causes a huge rise in the sea level. This is directly affected by global warming, which raises sea surface temperature (SST) (Anwar et al., 2024). In many coastal areas, the rate at which the shoreline is moving back is getting worse because of high wave energy and rising sea levels (Hasanah & Ranteallo, 2024; Zhou & Wang, 2024). The shore of Jepara Regency in Central Java directly faces the open seas of Java. Because of its location, the Jepara shore is especially vulnerable to wave energy during the westerly monsoon (Prathanazal et al., 2021; Putra et al., 2021). According to earlier studies, many Jepara coastal areas are very likely to have sediment deficits. This can lead to serious erosion in different places and in places with protected morphology that can absorb hydrodynamic energy (Ibrahim et al., 2023; Prathanazal et al., 2021; Putra et al., 2021; Sihotang et al., 2020).

Accurately quantifying multi decadal shoreline transformations requires robust spatial monitoring capable of capturing both gradual trends and episodic shifts across extensive coastal stretches (Damayanthi et al., 2025; Mbezi et al., 2024). The integration of multi temporal satellite imagery, such as the Landsat series, with Geographic Information Systems (GIS) and automated transect based tools like the Digital Shoreline Analysis System (DSAS) has become a standardized approach for evaluating historical coastal dynamics (Abdul Maulud et al., 2022; Facun et al., 2025; Himmelstoss et al., 2021a; Scala et al., 2024). Statistical metrics specifically End Point Rate (EPR), Net Shoreline Movement (NSM) and Shoreline Change Envelope (SCE) combined with rigorous positional uncertainty quantification, enable researchers to distinguish actual geomorphological shifts from sensor and tidal errors (Ayalke et al., 2023; Endarsih et al., 2025; Pratama et al., 2023). While recent studies in Jepara Regency have examined shoreline shifts over 10 year (2012–2021) and 30 year (1994–2024) periods (Ibrahim et al., 2023; Wahyudi & Apresia, 2025), a comprehensive 40 year analysis (1985–2025) that directly links multi decadal shoreline kinematics with long term hydrodynamic forcing and sea surface temperature anomalies remains unexplored.

Geographic information systems and remote sensing technologies have demonstrated significant efficacy in elucidating coastal change's long-term spatial and temporal patterns. End point rate (EPR), net shoreline movement (NSM), and shoreline change envelope (SCE) are analytical methodologies that utilize distance quantification techniques to accurately measure shoreline shift rates (Abdul Maulud et al., 2022; Endarsih et al., 2025; Pratama et al., 2023). This study quantifies the extent and rate of shoreline change over 40 years (1985–2025) and examines the impact of hydrodynamic conditions on the coastal stability of Jepara. The

findings of this study are anticipated to inform the development of suitable adaptation and mitigation strategies for sustainable coastal spatial management.

2. Methods

Research was conducted in the coastal waters of Jepara Regency, Central Java (Figure 1) along a 13 km stretch to observe coastline changes between 1985 and 2025. Spatial data were extracted using multi-temporal satellite imagery, incorporating datasets from Landsat 5 (TM) and Landsat 9 (OLI) (Damayanthi et al., 2025; Daswin Ebenezer & Kumar, 2023; Warnasuriya et al., 2018) to observe changes in the coastline from 1985 and 2025. The transect method is used to measure shoreline changes to calculate abrasion and accretion values. Each transect is 100 m apart. The baseline or reference line is drawn parallel to the beach and crosses it between 1985 and 2025. An ID number is assigned to the transect line that runs from the baseline to the beach, beginning north of the shoreline, every year. The transect length from the baseline to the shoreline was calculated using EPR, NSM, and SCE. The EPR method was developed by the United States Geological Survey (USGS) to calculate the rate of shoreline change (Thieler et al., 2009). The EPR method uses the following equation:

$$EPR = \frac{D_2 - D_1}{T_2 - T_1}$$

The NSM method is used to calculate the total displacement distance between the earliest (oldest) and latest (newest) shoreline positions on each transect (Himmelstoss et al., 2021b). The NSM equation used is as follows:

$$NSM = D_2 - D_1$$

The total distance between the shoreline position furthest from the baseline and the shoreline closest to the baseline on each transect was measured using the SCE method (Mutaqin, 2017). The equation used is as follows:

$$SCE = D_{max} - D_{min}$$

where D_2 is the distance of the most recent shoreline measured from the baseline, D_1 is the distance of the shoreline from the oldest year measured from the baseline, D_2 is the distance of the furthest shoreline measured from the baseline, D_1 is the distance from the nearest shoreline measured from the baseline, and T is the time of shoreline data collection. The calculation results for these three methods are presented to compare the results obtained for each method. The baseline was created following the coastal form's general pattern **(Figure 2)**. The transect lines were then drawn perpendicular to the coastline at uniform intervals along the study area (Facun et al., 2025; Scala et al., 2024). Next, the extent and rate of coastal spatial change were calculated by overlaying the 1985 coastline vector data with the 2025 coastline. The coastline shift distance was extracted by measuring the transect line segments' length between the coastline boundaries of the two time periods. The measurement results for each transect ID number were used to determine whether the coast was experiencing abrasion or accretion.

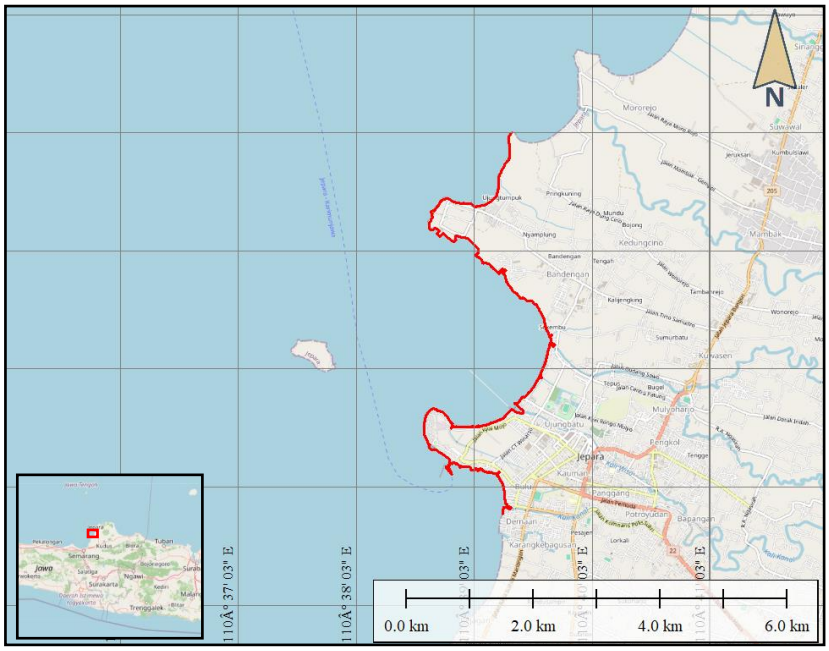


Figure 1. Map of research area in Jepara waters, Central Java

This study also analyzes the hydrodynamic conditions (tides, wave height, and period) that occurred from 1985 to 2025 in the waters of Jepara, Central Java, from 1985 to 2025. The tide dynamics, wave height, and period were calculated using the monthly average data of the European Center for Medium-Range Weather Forecasts satellite (Almar et al., 2023; Kumar et al., 2020). To facilitate descriptive analysis, data were analyzed using graphs and spatial maps

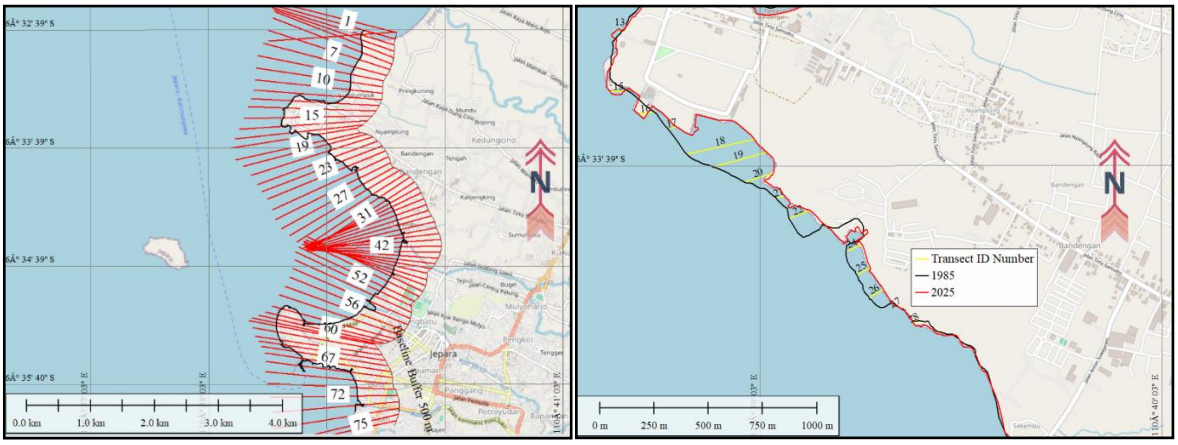


Figure 2. Use of the 100-meter transect method to calculate shoreline changes

Before the calculation of the methodological errors (End Point Rate or Net Shoreline Movement) the positional uncertainty (U_t) for every shoreline year must be determined. This value is calculated by means of Root Sum of Squares (RSS) method to account for various sources of error.The mathematical equation can be written as:

$$U_t = \sqrt{E_s^2 + E_d^2 + E_p^2 + E_t^2 + E_{sc}^2}$$ (Himmelstoss et al., 2021b)

Where: E_s^2 (georeferencing error): Error of rectification which is generated when aligning the imagery to real world coordinates, usually expressed as the Root Mean Square Error (*RMSE*) of the georeferencing process. E_d^2 (digitizing error): The operator error caused by manual line extraction. This is usually inferred from the width of the line on the screen. E_p^2 (pixel error): Error due to the spatial resolution of the satellite imagery. E_t^2 (tidal fluctuation error): The error due to the digitizing of shorelines under non-uniform tidal conditions. E_{sc}^2 (co-registration error): The error of spatial misalignment of images from different years (if applicable).

The End Point Rate (EPR) quantifies the speed of shoreline movement in meters per year. Consequently, to determine its uncertainty, the propagated NSM uncertainty must be divided by the temporal interval (in years) elapsed between the two respective shorelines (Hapke et al., 2006). The uncertainty formula for EPR is expressed as(Himmelstoss et al., 2021b):

$$U_{EPR} = \frac{U_{tA}^2 + U_{tB}^2}{Time_A + Time_b}$$

Net Shoreline Movement (NSM) and Shoreline Change Envelope (SCE) are metrics used to quantify absolute distances in meters. Because these analytical methods involve a comparison between two distinct shorelines (e.g shoreline A and shoreline B), the cumulative uncertainty is a statistical combination of the (U_t) values from both shorelines (Hapke et al., 2006). The uncertainty formula for NSM and SCE is calculated as (Himmelstoss et al., 2021b) :

$$U_{NSM} = U_{tA}^2 + U_{tB}^2$$

Where U_{tA}^2 represents the uncertainty of the initial shoreline, and U_{tB}^2 represents the uncertainty of the final or furthest shoreline.

3. Results and Discussion

Figure 3 shows an overlay of the 1985 shoreline vector digitization and the current 2025 circumstances in the Jepara coastal area. This image serves as the primary spatial database for calculating the coastal change distance. In the northern peninsula area (around Ujungtumpuk to the west coast of Bandengan), the red line

(2025) is more landward than the black line (1985). This indicates a significant coastline retreat over the past 40 years. In several segments in the central to southern parts (near the port), the red line (2025) appears to be more seaward. This pattern indicates an increase in land area, which could be triggered by high natural sedimentation rates (Kim et al., 2017; Li et al., 2014) or anthropogenic interventions such as the construction of coastal protection structures or reclamation (Wijaya & De Silva Nusantara, 2025; Y. Zhang & Hou, 2020).

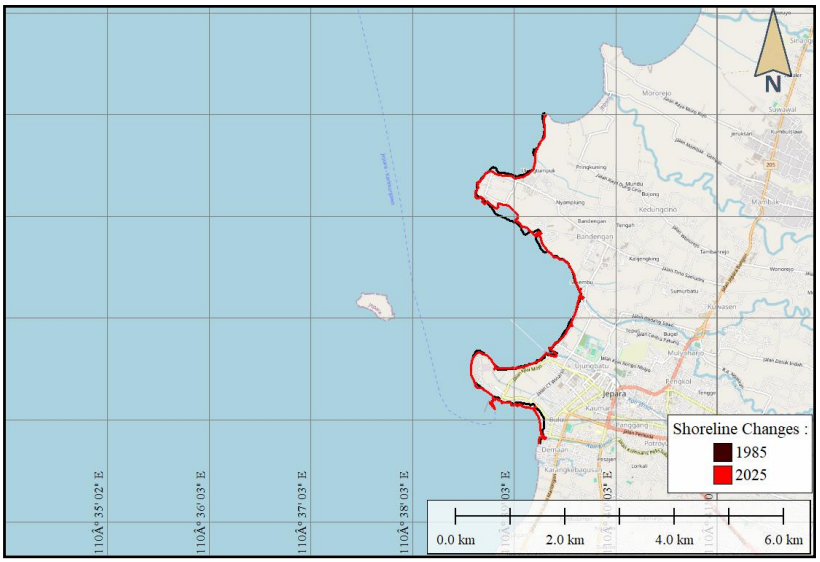


Figure 3. Digitized map of the coastline of Jepara, Central Java over the past 40 years (1985-2025)

Major shoreline changes occurred in the northern Jepara coast peninsula (**Figure 4**). This was observed in transects ID 1–20 (Ujungtumpuk area). The graph for this part shows a high negative value, which means that the coast is moving back at a rate of -8 to -9 meters per year. This high erosion rate indicates that the area is open to the constant flow of outside energy (Dail et al., 2000; Jackson et al., 2002). The shoreline pattern in the Jepara coastal area to the south is more stable. The mid-to-southern segment mostly changes in small amounts, with some positive values indicating that things are getting bigger. The coastline from Bandengan to Ujungbatu curves inward, making it look like a bay. This greatly weakens the littoral current (longshore current) energy. As the energy weakens, a deposition zone forms where sediment that has been eroded from the north is likely to settle (Kaliraj et al., 2014; May & Tanner, 2020; Zhang et al., 2023).

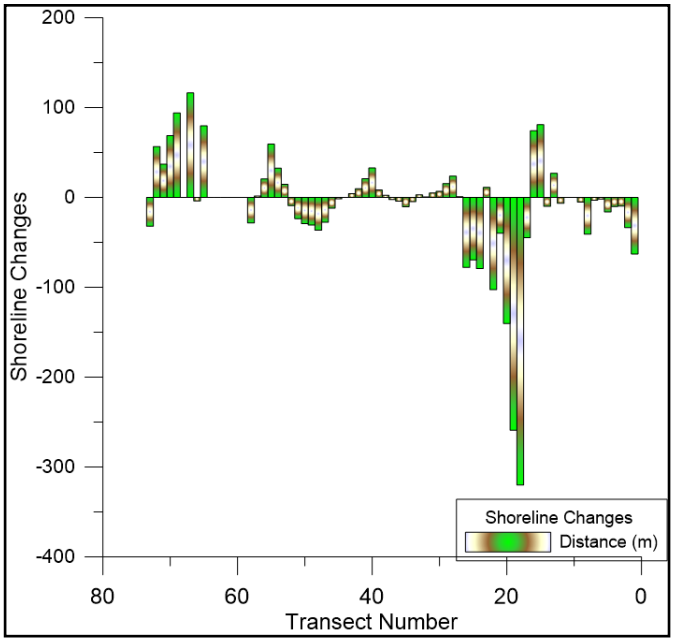


Figure 4. Length of transect of coastline changes in Jepara, Central Java over 40 years (1985-2025**)**

Massive abrasion conditions in the Ujungtumpuk peninsula area are quantitatively demonstrated by the much smaller length change in transects ID 18–22 (**Figure 5**). The northern region has significantly lost

sediment material over the past 40 years, as evidenced by the drop in EPR values to about -8 m/year and land retreat of more than -300 meters. Strong external pressure in this region strengthens the need for intervention to lower the abrasion rate. The point distribution of the graph in the Transect ID 30–55 range fluctuates extremely tightly around the value of 0. The spatial map of the Bandengan coastline area, which shows a very small area of changing polygons (both red and green), is compatible with these statistical findings.

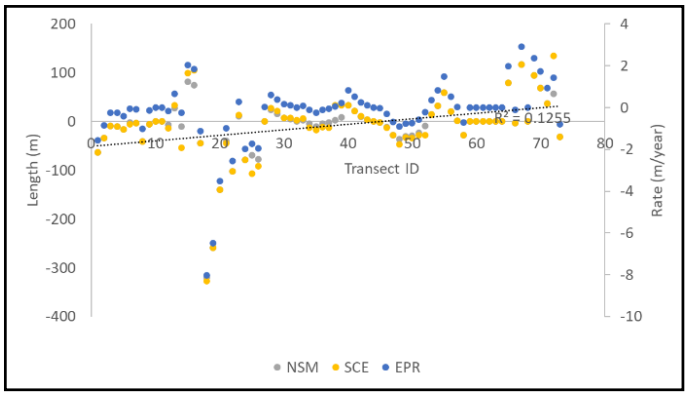


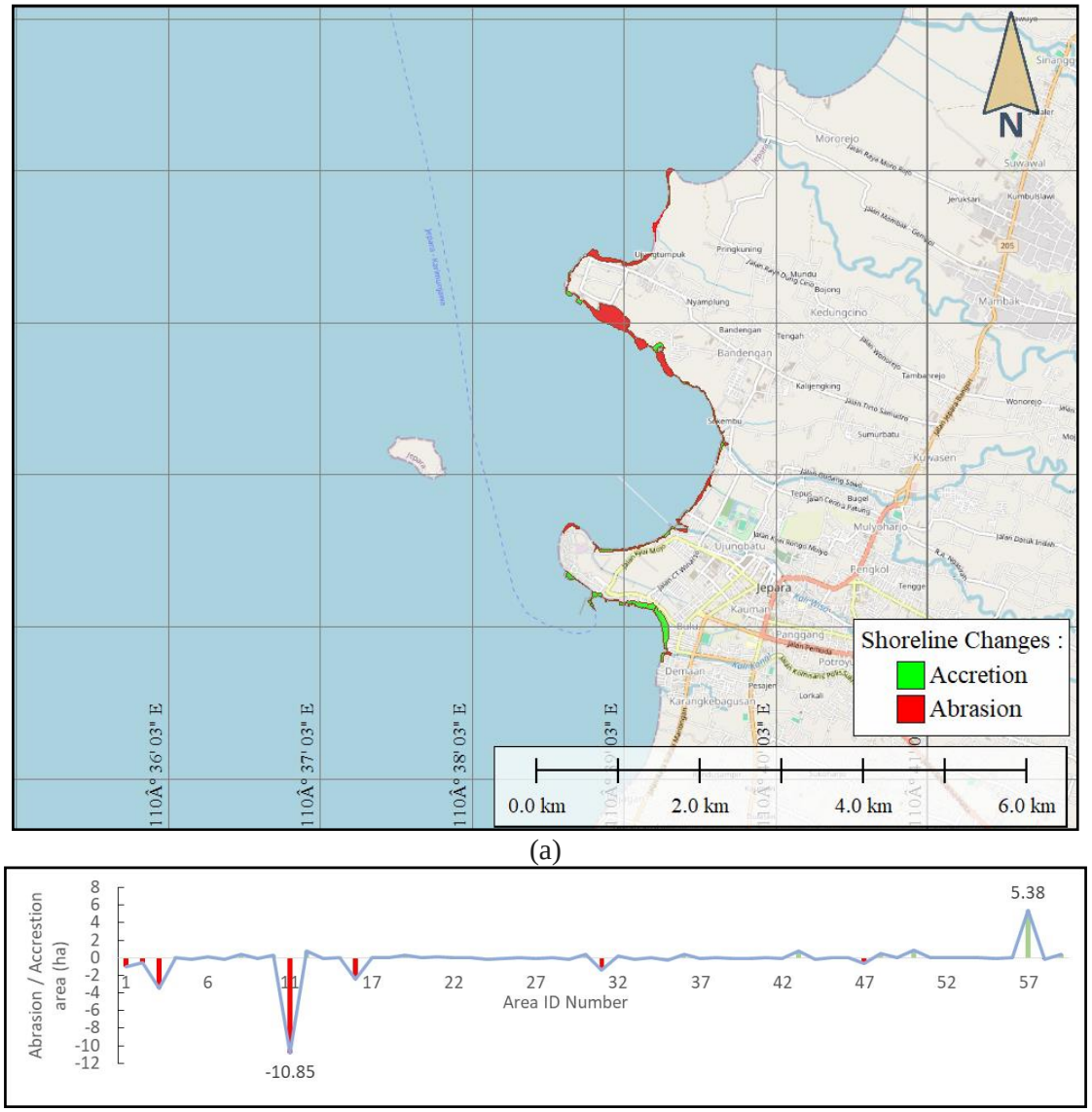
Figure 5. Results of measuring changes in coastline length using the NSM, SCE and EPR methods.

Land addition usually occurs in a few centrals to southern areas (closer to the coast of the city center/port of Jepara) and in a few coastal curves (small bays) that are more protected. The most likely cause of accretion in the area is longshore drift sediment transport, which then settles because the local hydrodynamic energy weakens or because artificial structures around the port trap the sediment (Laïbi et al., 2014; Putro & Lee, 2020). Curving bay formation can disperse the energy of littoral currents (longshore currents), thereby establishing a stable buffer zone and averting radical accretion and erosion. The green polygon (accretion) in the Ujungbatu area to the port center is directly associated with the sharp increase in EPR and NSM values in the Transect ID 60–75 range. The presence of efforts to preserve coastal conditions is demonstrated at the steady rate of increase in values1 to 2 m/year.

Figure 6 shows the extent to which the dynamics of shoreline change have affected the coastal area of Jepara. The picture shows the results of taking polygons from the overlay process between the 1985 and 2025 shorelines. These polygons are then divided into two groups: abrasion and accretion. The headland area that sticks out into the sea loses the most land, especially in the north (Ujungtumpuk area). This event shows that the headland area on the Jepara coast is always exposed to external forces for a long time, causing sedimentary material to erode (Fitri et al., 2019; Green & Coco, 2014).

Quantitative data analysis revealed an imbalance between abrasion and accretion in Jepara's coastal waters. Based on observation data from 58 points, the Jepara coast generally experienced land shrinkage. Abrasion events were recorded as dominant at 31 observation points, whereas accretion only occurred at 27 points. The most extreme and destructive abrasion occurred in Area ID 11, where land eroded by -10.85 hectares. Other critical abrasion points occurred in Area ID 3, which lost -3.44 hectares of land, and Area ID 16, which lost -2.45 hectares. The largest land gain or accretion occurred in Area ID 57, with an additional area of 5.38 ha. Areas ID 50 and ID 43 experienced accretion of 0.85 and 0.77 hectares, respectively. If accumulated, the total land area lost due to abrasion from all observation points reached -22.33 hectares. The total land area formed through accretion is only 10.15 hectares. This indicates a net coastal area shrinkage of approximately 12.18 ha. The average land area lost at each abrasion point is approximately -0.72 hectares, which is almost twice as large as the average land gain at each accretion point, which is only approximately 0.37 ha. These data indicate that external, destructive forces are acting much more strongly than natural land formation processes (Arnall, 2023; Asmal et al., 2024; Wright & Thom, 1977).

Based on wave data, the two main wind directions are northeast (the east monsoon) and northwest (the west monsoon). Approximately 35.4% of the data collected over the last 40 years comes from waves from the northwest and west (**Figure 7**). In these directions, large waves are the most common. The largest wave from the northwest is 2.94 m, and the average wave height is 0.66 m. The data show that the west monsoon, which lasts from December to February, is when most high waves occur. Strong winds blowing across the open Java Sea (a long fetch area) create high waves that could be dangerous in the surrounding waters (Miranda et al., 2023; Prasita et al., 2022).



(a)

(b)

Figure6. (a) Map abrasion and accretion area and (b) coastline change value from 1985 to 2025

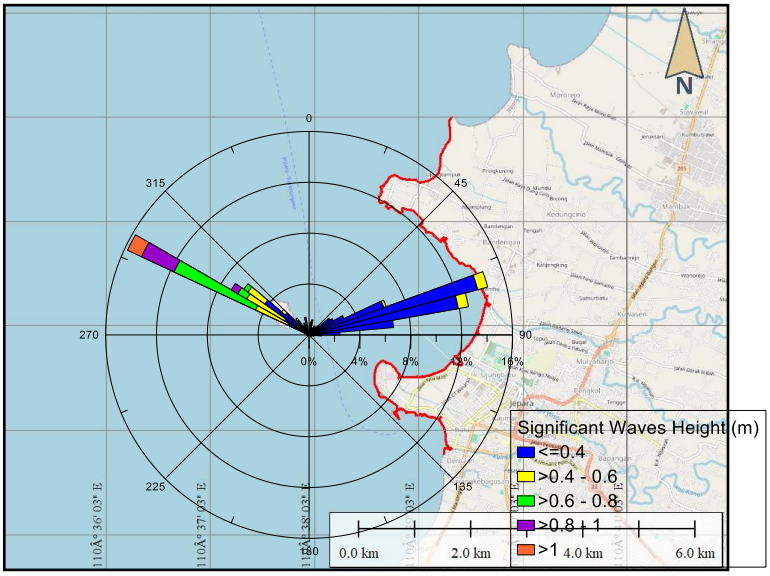


Figure 7. Rose diagram of significant waves in the waters of Jepara, Central Java over the past 40 years (1985-2025)

Waves from the east and northeast have made up approximately 37.1% of the total data in the last 40 years (11.3% from the east and 25.8% from the northeast). Waves coming from the east and northeast will have a smaller or lower range than those coming from the west and northwest. The highest wave height recorded from this direction is only 1.12 m, and the average is only 0.33 m. These waves mostly occur during the East Monsoon, which runs from June to August.

The wind is usually steady and comes from the east, but Jepara's waves are usually calmer than those in the West Monsoon. This is because the islands east of the Java Sea block the wind and the monsoon conditions are drier (Barokah et al., 2023). The wave period was between 3.9 s and 4.3 s. This information shows the characteristics of medium-frequency waves that are usually observed in wind-affected waters. There were not many changes from time to time. For example, on January 1, 1985, the wave period started at 4.26 s in the morning and dropped to 4.0 s in the afternoon (**Figure 8**). The wave period stayed steady at 4 s, which means that the sea conditions were not very stormy, which would normally cause the period value to increase significantly (swell waves). A 4-s wave period indicates that small waves have the greatest effect on Jepara waters. An abrupt increase in this period to 8–12 s indicates the onset of swell waves (Ardhuin et al., 2009).

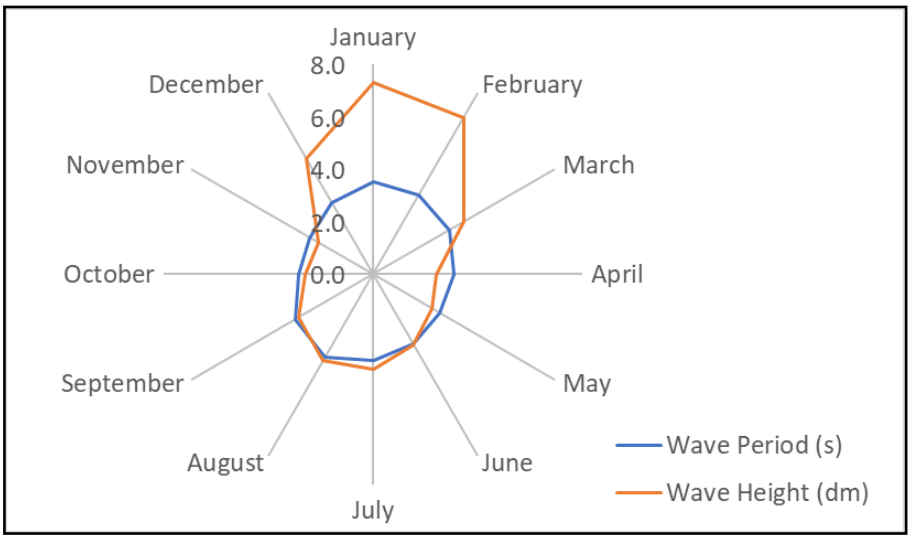
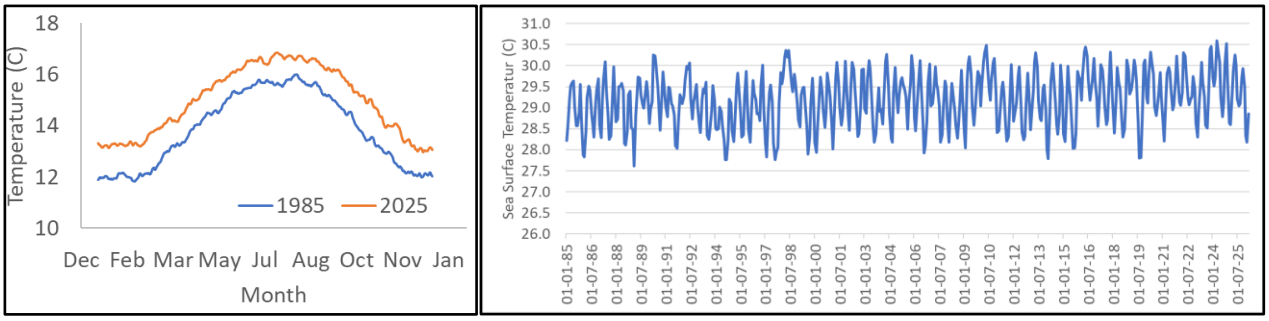


Figure 8. Monthly Averages of Significant Wave Height and Period (1985–2025)

Shoreline change is a dynamic hydro morphological process, conditioned by complex interactions between regional oceanographic driving forces (mainly wave energy) and local coastal environmental characteristics (Sakka et al., 2025). Analysis of historical data of offshore significant wave heights (SWH) reveals that ocean waves are the main driving agent to generate longshore currents and initiate sediment transport. Although offshore wave height parameters are perceived relatively constant and fluctuate stably in the long term, the observed spatial heterogeneity in End Point Rate (EPR) values over the observation transects is remarkably high, from conditions of massive coastal erosion to significant land accretion processes.

This phenomenon shows that the offshore wave height is not the sole factor controlling the rate of shoreline fluctuation. The local rates of erosion and accretion are primarily governed by boundary factors that modify wave energy in its journey toward shallow waters (nearshore) (Asri & Novita Sari, 2023). These are the differences in the local bathymetric profiles that control the degree of shoaling and refraction of the waves, the geomorphological orientation of the shoreline with respect to the incident wave angle and the dynamics of the surrounding littoral sediment supply. The correlation between offshore waves and EPR is thus not a linear homogeneous relation but a spatial relation strongly modulated by the physical conditions of the seabed and the coast at each respective shoreline segment.



(a) (b)

Figure 9. Graph of sea surface (a) monthly and (b) annualy temperature over 40 years (1985-2025)

The sea surface temperature continuously changes. The lowest temperatures are between 27.5℃ and 28.5℃, and the highest temperatures are between 29.5℃ and 30.5℃ (**Figure a**). There is a trend of rising temperatures; the highest temperatures rarely exceeded 30.5℃ in the 1980s and 1990s. Between 2010 and 2025, many more days were observed when the temperature reached or exceeded 30.5℃. The most notable peaks occurred in 2010, 2016, and 2023-2025. Several extreme temperature spikes have been recorded, particularly in 1997–1998, 2015–2016, and around 2024/2025. These spikes are probably linked to global weather events like El Niño, which raises sea surface temperatures in many marine areas, including Indonesia (Prasetyo & Nabilah, 2017; Sekaranom, 2023). These drops usually occur during periods of strong winds and upwelling or when heavy rainfall occurs. A steady rise in temperature is a major indicator of global climate change (Lindsey & Dahlman, 2020; Sobrino et al., 2020). Oceans absorb extra heat that greenhouse gases keep in the Earth's atmosphere. This process gradually increases the temperature of the ocean surface. A comparison of the average daily global surface air temperature at a height of 2 m between 1985 and 2025 indicates global warming (**Figure 9b**). Temperatures in 2025 are consistently above those in 1985, with a daily increase margin ranging from 1℃ to exceeding 1.5℃ per month. For example, the lowest point in global temperatures at the beginning of the year, which was previously around 12℃ in 1985, escalated to exceed 13℃ in 2025. Furthermore, the peak global surface air temperature, which generally occurs in the middle of the year, has also increased.

The maximum daily temperature, which was 16℃ in 1985, has now risen to nearly 17℃ by 2025. This drastic increase in surface air temperature anomalies has direct implications for increasing ocean temperatures, which then triggers a thermal expansion process in water volume and contributes significantly to sea level rise (Liang et al., 2025) on a regional scale, such as in the waters of Jepara, Central Java. Sea level rise due to thermal expansion of sea surface temperatures makes the coastal areas of North Java, including Jepara, increasingly vulnerable. Higher sea levels cause waves to have a longer inland reach (Dodet et al., 2019; Laignel et al., 2023). In addition to abrasion, this condition increases the frequency and severity of tidal flooding that often occurs in Java's northern coastal areas.

Table 1. Error source parameters for multitemporal shoreline extraction

Error Parameter	Landsat 5 TM (1985)	Landsat 9 OLI-2 (2026)	Justification for Value Assignment
Pixel Resolution	30 m	30 m	Extraction utilizing conventional multispectral bands
Georeferencing / Rectification	12 m	5 m	Historical imagery exhibits a higher rectification RMSE; Landsat 9 utilizes high-precision Level-1TP data.
On-screen Digitization	2 m	2 m	Estimation of operator visual variance and cursor thickness during on-screen delineation.
Tidal Fluctuation	5 m	5 m	Assumption of horizontal shift at the land-water interface due to tidal variations on a gently sloping coastal geomorphology.

In this study, the Total Positional Uncertainty (TPU) of shoreline extraction was calculated based on the standards of the United States Geological Survey (USGS). The uncertainty quantification includes different possible error sources (variance) of the applied multitemporal remote sensing instruments. The error

parameters for the initial (Landsat 5 TM) and final (Landsat 9 OLI-2) imagery were defined based on the sensor resolution, geometric accuracy, and local oceanographic conditions, and are summarized in Table 1. For each shoreline the TPU value was determined using the root sum of squares of all individual error variables. The positional uncertainty for the initial shoreline $(U_{t(L5)})$ was then determined according to this formulation to be 32.76 m. The recent shoreline, on the other hand, has a slightly lower uncertainty level $(U_{t(L9)})$ of 30.89 m. The next step is to propagate these individual errors to characterize the total margin of error for the statistical measures of shoreline change over the 40-year observation period . The total uncertainty for absolute distance-based metrics, Net Shoreline Movement and Shoreline Change Envelope, was derived as:

$$U_{NSM/SCE} = \sqrt{U_{t(L5)}^2 + U_{t(L9)}^2} = \sqrt{1073 + 954} \approx \pm 45.02\ m$$

The uncertainty in the annualized rate of shoreline change, as quantified by the End Point Rate, was further calculated as the total absolute distance uncertainty divided by the observed temporal span (Δt= 40 years):

$$U_{EPR} = \frac{U_{NSM/SCE}}{\Delta t} = \frac{45.02}{40} \approx \pm 1.13\ m/year$$

This overall margin of error, from both the rate and distance metrics, is then incorporated to account for the validity of the physical coastal vulnerability parameter weighting in the overall index analysis.

4. Conclusion

Shoreline changes in the coastal waters of Jepara Regency have shown a clear land erosion trend over the last 40 years. This is because destructive external factors have had a greater effect than natural land formation processes. Statistically, the coastline is getting smaller because the amount of land lost to erosion is much greater than the amount of land gained by accretion. The most severe abrasion damage occurred in the northern headland area. This is because during the West Monsoon, the winds blow from the west to the northwest. Land expansion occurs along the bay's morphological curve in the middle and southern parts. The rate at which the coastline is moving back is getting worse because of global warming, as evidenced by the fact that sea surface temperatures are reaching critical levels more often

Reference

Abdul Maulud, K. N., Selamat, S. N., Mohd, F. A., Md Noor, N., Wan Mohd Jaafar, W. S., Kamarudin, M. K. A., Ariffin, E. H., Adnan, N. A., & Ahmad, A. (2022). Assessment of Shoreline Changes for the Selangor Coast, Malaysia, Using the Digital Shoreline Analysis System Technique. *Urban Science*, *6*(4). https://doi.org/10.3390/urbansci6040071

Almar, R., Boucharel, J., Graffin, M., Abessolo, G. O., Thoumyre, G., Papa, F., Ranasinghe, R., Montano, J., Bergsma, E. W. J., Baba, M. W., & Jin, F. F. (2023). Influence of El Niño on the variability of global shoreline position. *Nature Communications*, *14*(1). https://doi.org/10.1038/s41467-023-38742-9

Anwar, I. P., Setiawan, A., Herho, S. H. S., Atmojo, A. T., & Khadami, F. (2024). Analisis Parameter Laut-Atmosfer terhadap Anomali Tinggi Muka Air di Laut Jawa. *Indonesian Journal of Oceanography*, *6*(4), 306–315. https://doi.org/10.14710/ijoce.v6i4.24645

Asri, H., & Novita Sari, F. (2023). Monitoring Coastal Line Changes Using the Digital Shoreline Analysis System (DSAS) Method in the Coastal Area of Mekkatta Village, Mejene Regency. *Jurnal IPTEKS Pemanfaatan Sumberdaya Perikanan*, *10*(2), 107–118. https://journal.unhas.ac.id/index.php/iptekspsp/article/view/32060

Ayalke, Z. G., Şişman, A., & Akpinar, K. (2023). Shoreline extraction and analyzing the effect of coastal structures on shoreline changing with remote sensing and geographic information system: Case of Samsun, Turkey. *Regional Studies in Marine Science*, *61*, 102883.

Damayanthi, I. D. A. M., Pujianiki, N. N., & Tonyes, S. G. (2025). Cloud-based multitemporal shoreline change analysis using google earth engine and DSAS: A case study of Canggu Beach, Bali, Indonesia. *Journal of Infrastructure Planning and Engineering*, *4*(2), 83–91. https://doi.org/10.22225/jipe.4.2.2025.83-91

Daswin Ebenezer, M., & Kumar, M. (2023). Coastline change rate estimation on the southern coastal districts of Tamil Nadu, India using the multi temporal google earth images and GIS based statistical approach. *Global Nest Journal*, *25*(4), 95–103. https://doi.org/10.30955/gnj.004482

Endarsih, A. E., Kurniasih, A., & Khomarudin, M. R. (2025). Analisis Perubahan Garis Pantai Menggunakan Digital Shoreline Analysis System untuk Mendukung Mitigasi Pesisir Kota Pekalongan, Jawa Tengah. *Jurnal Teknologi Lingkungan*, *26*(1), 019–030. https://doi.org/10.55981/jtl.2025.3960

Facun, L. P., Sta Maria, M. Y., Ducao, R., Clemente, J. J., Carmelo, E. M., Maon, A., Malaya, A. R., Cuison, F., & Siringan, F. (2025). QGIS Shoreline Change Analysis Tool (QSCAT): A fast, open-source shoreline change analysis plugin for QGIS. *Environmental Modelling and Software*, *184*. https://doi.org/10.1016/j.envsoft.2024.106263

Hasanah, M. N., & Ranteallo, I. R. (2024). Antisipasi Dampak Kenaikan Muka Air Laut Dan Mitigasinya Pada Kawasan Pantai Galesong Takalar. *Riset Sains Dan Teknologi Kelautan*, 78–85. https://doi.org/10.62012/sensistek.v7i1.31671

Himmelstoss, E. ., Henderson, R. ., Kratzmann, M. ., & Farris, A. . (2021a). *Digital Shoreline Analysis System (DSAS) Version 5 . 1 User Guide*. https://pubs.usgs.gov/publication/ofr20211091

Himmelstoss, E. A., Henderson, R. E., Kratzmann, M. G., & Farris, A. S. (2021b). Digital Shoreline Analysis System (DSAS) Version 5.1 User Guide: U.S. Geological Survey Open-File Report 2021–1091. *U.S. Geological Survey*, *2021–1091*, 104. https://doi.org/10.3133/ofr20211091

Ibrahim, M. L. G., Atmodjo, W., & Widada, S. (2023). Perubahan Garis Pantai Perairan Teluk Awur Kabupaten Jepara Menggunakan DSAS (Digital Shoreline Analysis System) Dari Tahun 2012 Sampai 2021. *Indonesian Journal of Oceanography*, *5*(2), 198–206. https://doi.org/10.14710/ijoce.v5i2.16519

Irsadi, A., Martuti, N. K. T., Abdullah, M., & Hadiyanti, L. N. (2022). Abrasion and Accretion Analysis in Demak , Indonesia Coastal for Mitigation and Environmental Adaptation. *Nature Environment and Pollution Technology*, *21*(2), 633–641. https://doi.org/https://doi.org/10.46488/NEPT.2022.v21i02.022

Kumar, L., Afzal, M. S., & Afzal, M. M. (2020). Mapping shoreline change using machine learning: a case study from the eastern Indian coast. *Acta Geophysica*, *68*(4), 1127–1143. https://doi.org/10.1007/s11600-020-00454-9

Mbezi, J., Mango, J., Lubida, A., Valerian, R., & Kato, L. (2024). Exploring shoreline changes and their implications in coastal communities using GIS and remote sensing techniques: The case of eastern beaches of Unguja island, Tanzania. *Regional Studies in Marine Science*, *75*, 103566.

Mutaqin, B. W. (2017). Shoreline changes analysis in kuwaru coastal area, yogyakarta, Indonesia: An application of the digital shoreline analysis system (DSAS). *International Journal of Sustainable Development and Planning*, *12*(7), 1203–1214. https://doi.org/10.2495/SDP-V12-N7-1203-1214

Ondara, K., Rahmawan, G. A., Gemilang, W. A., Wisha, U. J., & Dhiauddin, R. (2018). Numerical hydrodynamic wave modelling using spatial discretization in Brebes waters, Central Java, Indonesia. *International Journal on Advanced Science, Engineering and Information Technology*. https://doi.org/10.18517/ijaseit.8.1.4166

Ondara, K., Wisha, U. J., Dhiauddin, R., & Purnawan, S. (2022). Concentration of dissolved heavy metal around the Rupat waters industrial activity, Malacca Strait. *E3S Web of Conferences*, *339*. https://doi.org/10.1051/e3sconf/202233902009

Pratama, R. Y., Sulaksana, N., Sukiyah, E., Iskandarsyah, T. Y. W. M., Novico, F., Zulfahmi, Z., Sudjono, E. H., & Ranawijaya, D. (2023). Short-Term Coastal Landscape Evolution In Cirebon Bay Using Coastline Environment Analysis. *Journal of Environmental Engineering and Landscape Management*, *31*(3), 186–195. https://doi.org/10.3846/jeelm.2023.19468

Prathanazal, N. M., Sasmito, B., & Sabri, L. M. (2021). Analisis Kerentanan Daerah Pesisir Kabupaten Jepara Menggunakan Coastal Vulnerability Index (CVI). *Geodesi Undip*, *10*(1), 115–123.

Putra, T. W. L., Zainuri, M., & Sugianto, D. N. (2021). Studi Penjalaran Gelombang Laut di Pulau Panjang, Kabupaten Jepara. *Buletin Oseanografi Marina*, *10*(1), 75–87. https://doi.org/10.14710/buloma.v10i1.34299

Riptanti, E. W., Harisudin, M., Kusnandar, Khomah, I., Setyowati, N., & Qonita, R. R. A. (2025). Examining the Impact of Abrasion on the Livelihood of Fishermen and Aquaculture Farmers: Empirical Study on the North Coast of Central Java Province. *International Journal of Sustainable Development and Planning*, *20*(6), 2509–2518. https://doi.org/10.18280/ijsdp.200619

Sakka, Assegaf, A. H., Amiruddin, Saaduddin, Azis, S. N. A. A., & Ismail, A. M. I. (2025). Impact of wave energy and sediment transport on shoreline changes: A multi-temporal satellite image analysis in Galesong, Takalar Regency, Indonesia. *Journal of Degraded and Mining Lands Management*, *12*(4), 8179–8189. https://doi.org/10.15243/jdmlm.2025.124.8179

Scala, P., Manno, G., & Ciraolo, G. (2024). Coastal dynamics analyzer (CDA): A QGIS plugin for transect based analysis of coastal erosion. *SoftwareX*, *28*. https://doi.org/10.1016/j.softx.2024.101894

Sihotang, D. G., Setiyono, H., Subardjo, P., Satriadi, A., Hariyadi, H., Widiaratih, R., & Rifai, A. (2020). Sedimentasi dan Abrasi di Pantai Bandengan, Kabupaten Jepara. *Indonesian Journal of Oceanography*, *2*(4), 334–340. https://doi.org/10.14710/ijoce.v2i4.8579

Solihuddin, T., Husrin, S., Salim, H. L., Kepel, T. L., Mustikasari, E., Heriati, A., Ati, R. N. A., Purbani, D.,

Mbay, L. O. N., Indriasari, V. Y., & Berliana, B. (2021). Coastal erosion on the north coast of Java: Adaptation strategies and coastal management. *IOP Conference Series: Earth and Environmental Science*, *777*(1). https://doi.org/10.1088/1755-1315/777/1/012035

Thieler, E. R., Himmelstoss, E. ., Zichichi, J. ., & Ergul, A. (2009). DSAS 4.0 Installation Instructions and User Guide. In *U.S. Geological Survey Open-File Report 2008-1278* (Vol. 3, pp. 291–294). http://pubs.usgs.gov/of/2008/1278/

Umar, H., Paotonan, C., Rachman, T., Nur, S. H., Muhiddin, A. H., Maming, M. I., Rezky Andriadi, A. M., & Assidiq, F. M. (2025). Assessing Sediment Transport and Shoreline Dynamics in High-Energy Tropical Coasts. *Civil Engineering Journal (Iran)*, *11*(7), 3020–3038. https://doi.org/10.28991/CEJ-2025-011-07-022

Wahyudi, N. R., & Apresia, F. (2025). Shoreline change detection in Jepara regency, Indonesia, using multitemporal Landsat imagery from 1994 to 2024. *Ecological Engineering & Environmental Technology*, *26*(11), 361–374.

Warnasuriya, T. W. S., Gunaalan, K., & Gunasekara, S. S. (2018). Google Earth: A New Resource for Shoreline Change Estimation—Case Study from Jaffna Peninsula, Sri Lanka. *Marine Geodesy*, *41*(6), 546–580. https://doi.org/10.1080/01490419.2018.1509160

Zhou, M., & Wang, S. (2024). The risk of concurrent heatwaves and extreme sea levels along the global coastline is increasing. *Communications Earth and Environment*, *5*(1). https://doi.org/10.1038/s43247-024-01274-1